PCP
PLANT & CELL PHYSIOLOGY

Regular Paper

Chlorophyll Fluorescence and Reflectance-Based Non-Invasive Quantification of Blast, Bacterial Blight and Drought Stresses in Rice

David Šebela[1,2,3], Cherryl Quiñones[3], Casiana V. Cruz[3], Isabelita Ona[3], Julie Olejníčková[1] and Krishna S.V. Jagadish[3,4,*]

[1]Global Change Research Institute CAS, 603 00, Brno, Czech Republic
[2]Faculty of Science, University of South Bohemia, 37005, České Budějovice, Czech Republic
[3]International Rice Research Institute, DAPO BOX 7777, Metro Manila, Philippines
[4]Department of Agronomy, 2004 Throckmorton Plant Science Center, Kansas State University, Manhattan, KS 66506, USA
*Corresponding author: E-mail, kjagadish@ksu.edu
(Received October 4, 2016; Accepted September 6, 2017)

Response of rice (*Oryza sativa*) exposed to both biotic and abiotic stresses can be quantified by employing fast and accurate optical methods. In this study, the overall stress responses of (i) 12 near-isogenic lines (NILs) in the genetic background of the rice blast-susceptible cultivar Lijiangxintuanheigu (LTH) and (ii) four NILs in the genetic background of the bacterial blight-susceptible cultivar IR24, were inspected by means of Chl fluorescence (Chl-F) imaging. The distribution of the maximum and effective quantum yield of PSII (Fv/F_M and QY) and steady-state Chl-F (Ft) were found to be effective in differentiating symptomatic leaf tissue for both rice blast and bacterial blight, which correlated well with 30 cycles of rice blast and six cycles of bacterial blight previously screened using classical (manual) approaches. Subsequently, identified Chl-F parameters allowing detection under ambient light (QY and Ft) were tested across both biotic and abiotic (drought) stress experiments, for rice cultivars contrasting for drought stress response (N22, IR64 and NSIC Rc 222). Their applicability has been proven for both rice blast and bacterial blight; however, QY failed to detect the effect of drought. In addition to Chl-F, the usefulness of 11 selected vegetation indices (Vis) was tested on these three cultivars exposed to particular stresses: (i) rice blast was detectable by Vis calculated from the visible spectrum; (ii) bacterial blight by near-infrared-related Vis; and (iii) drought by Vis calculated from the visible spectrum. The key Chl-F parameters and/or Vis have been summarized and discussed.

Keywords: Bacterial blight • Chlorophyll fluorescence • Drought stress • Reflectance • Rice bast.

Abbreviations: BB, bacterial blight; Chl-F, chlorophyll fluorescence; DAI, days after inoculation; NDM, non-destructive measurement; NIL, near isogenic line; NIR, near infrared; PRI, photochemical reflectance index; RB, rice blast; Vi, vegetation index; *Xoo*, *Xanthomonas oryzae* pv. *Oryzae*.

Introduction

Geographically, rice is the most widely cultivated cereal (Khush 2005) and hence is exposed to a range of environmental challenges. Rice grown in tropical and subtropical ecosystems is frequently challenged by drought, which is considered to be a major abiotic stress (Wassmann et al. 2009, Jagadish et al. 2012), and biotic stresses such as rice blast (RB; Babujee and Gnanamanickam 2000) and bacterial blight (BB; Mew 1987, Cottyn and Mew 2004), significantly reducing rice yields. Global climate change models predict much greater variability with precipitation patterns and temperature, leading to a drier and warmer climate (IPCC 2013), accompanied by intensified pest and disease pressure (Walther et al. 2002). Rice responses to such abiotic and biotic stresses are highly complex and involve intricate changes in plant responses. Many research studies have highlighted precise and repeatable phenotyping for the above-mentioned stresses to be a serious challenge (White et al. 2012, Fiorani and Schurr 2013). Among others, drought stress phenotyping is complicated by additional noise added due to strong interactions with other environmental factors such as temperature and relative humidity, while estimating the impact of biotic stresses is challenged by tedious manual estimations generally prone to errors.

Drought stress regularly affects about 23 Mha of rice land, having serious consequences on the agricultural gross domestic product (Pandey et al. 2007). It is by far the most devastating abiotic stress affecting rice cultivation, which can potentially occur at any time throughout the crop growth cycle. However, its occurrence during the critical flowering and early grain-filling stages is known to be highly damaging (Suriyan et al. 2010, Rang et al. 2011). The major limitation during terminal drought stress is the lack of water to allow normal transpiration, resulting in limited Chl function, reduced photosynthetic capacity and poor carbon assimilation (Hatch and Slack 1970, Centritto et al. 2009, Gu et al. 2012).

Plant Cell Physiol. 59(1): 30–43 (2018) doi:10.1093/pcp/pcx144, Advance Access publication on 9 October 2017, available online at www.pcp.oxfordjournals.org

Among biotic stresses, RB (Babujee and Gnanamanickam 2000) and BB (Mew 1987) are two highly damaging rice diseases. RB caused by *Magnaporthe oryzae* (anamorph: *Pyricularia oryzae*) causes lesions on all parts of the plant, including seeds, pedicles, panicles, panicle neck, leaf collars and leaves. The most common symptom (Devi and Sharama 2010) that is routinely analyzed, however, occurs on the leaves. BB caused by *Xanthomonas oryzae* pv. *oryzae* (*Xoo*) affects both irrigated and rainfed rice, resulting in 20–50% yield reduction (Gnanamanickam et al. 1999). So far, >30 BB resistance genes (*Xa1*–*Xa37t*) have been identified (Khush and Angeles 1999, Chu et al. 2006a, Chu et al. 2006b).

In principle, the abiotic and biotic stress factors mentioned above can alter several physiological processes, of which changes in pigment composition and subsequently photosynthesis are most critical. A reduction in Chl content on exposure to either abiotic or biotic stresses has been reported in several plant species, as well as in rice (Chutia and Borah 2012). Such a decrease in photosynthetic pigment content and the associated metabolic changes affect the optical properties of leaves. Several optical signals, acting as reporters of the physiological status of the plants, have frequently been used for quantifying abiotic stress as well as for monitoring biotic stress (Chaerle and Van Der Straeten 2000).

Employing Chl fluorescence (Chl-F) provides fast and accurate, non-invasive insight into stress-induced photosynthetic damage in plants, since its emissions can be correlated with photosynthetic rates (Krause and Weiss 1991). A large number of different Chl-F parameters with known physiological interpretation (Maxwell and Johnson 2000) have been calculated in the past and are frequently used across plant species. Only a few studies have used this approach to quantify the impact of abiotic stress on rice [e.g. nutrient stress (Subhash and Mohanan 1994), salt stress (Moradi and Ismail 2007), chilling stress (Y.H. Zhang et al. 2010) and water stress (Sikuku et al. 2010)], while its application in rice biotic stress quantification has not been documented. Specifically, Chl-F imaging provides an opportunity to investigate RB and BB experimentally; RB and BB can reduce photosynthesis not only in the infected leaf spots, but also in immediately surrounding plant tissue, depending on the susceptibility of the cultivars (Bastiaans 1991).

Ch-F can be a very powerful tool to study stress-induced photosynthetic activity, when coupled with other non-invasive techniques, e.g. reflectivity of leaf tissue. Leaf pigments absorb various amounts of light at different wavelengths and, thus, leaf reflectance is strongly dependent on their content. The concentration of these pigments (e.g. Chl and carotenoids) reflects the efficiency of a plant to utilize photosynthetically active radiation for biosynthetic processes, and is thus strongly related to the physiological status of the plant. Leaf optical characteristics as a response to plant stresses have been investigated across different abiotic stresses including heat and water stress (e.g. Ceccato et al. 2001), and biotic stresses among certain plant species [e.g. sugar beet (Mahlein et al. 2012)], with only a few reports related to rice. Kobayashi et al. (2003) reported the multispectral index with the maximum sensitivity to leaf blast regardless of the disease severity. As RB disease severity increased, changes of reflectance in the region attributed to Chl/carotenoid content, and the near-infrared (NIR) region were also monitored by H. Zhang et al. (2010). NIR reflectance was also identified as the best indicator for BB (Yang 2010) and drought stress in rice. Drought stress-sensitive, NIR-related indices (Penuelas et al. 1993) were inspected across species; however, reflectance in this visible region is affected primarily by the leaf structure. Thus, for more complex high-throughput screening of both biotic and abiotic stresses, the reflectance in the visible region (determined mostly by photosynthetic pigments) is the major bottleneck.

The severity and significance of damage caused by both biotic and abiotic stresses have necessitated the development of different fast and accurate strategies to reduce crop losses. To facilitate investigations and to identify stress-tolerant and susceptible sources of rice accessions from a diverse set of germplasm, non-invasive phenotyping techniques need to be developed and standardized. Hence, the major objectives of our studies were to (i) detect and compare the impact of RB and BB on rice accessions differing in their response to these stresses by comparing routine manual scoring with a Chl-F imaging system; (ii) test Chl-F parameters identified by the imaging system for temporal detection of RB and BB under ambient light conditions; and (iii) compare applicability of these Chl-F parameters together with selected vegetation indices (Vis) across both biotic (RB and BB) and abiotic (drought) stresses, under greenhouse and field conditions.

Results

Traditional manual screening of RB and BB

Our results revealed substantial genotypic variation among the investigated cultivars in terms of resistance/susceptibility to RB and BB. Classical severity screening is based on the visual evaluation of pathogen spread through the inoculated leaf or plant population and its progress over time. To support our findings, previous severity screenings are overlaid in **Fig. 1**. Grey columns (**Fig. 1A**) represent means of classical diseased leaf area screenings (%) obtained during 30 consecutive cycles of screening for RB at 15 days after inoculation (DAI); gray and white columns (**Fig. 1B**) represent means of lesion length (cm) obtained during six consecutive cycles of classical BB severity screening at 5 DAI for both *PXO61* and *PXO99* strains; while the black diamonds show the representative mean values from our study obtained during the wet season in 2013. Means for both experiments (**Fig. 1**) showed a clear trend with positive correlation [($R^2 = 0.55$, $P < 0.05$ for all near-isogenic lines; NILs; ($R^2 = 0.95$, $P < 0.01$ after excluding those responding contrastingly, i.e. IRBL5, IRBL6 and IRBL8)] between previous and present observations (**Fig. 1A**), and an even stronger correlation ($R^2 = 0.85$, $P < 0.01$) between the six cycles of manual screening and the current study in the case of BB (**Fig. 1B**). The highest average diseased leaf area during 30 cycles of RB (**Fig. 1A**) was found in the susceptible cultivar Lijiangxintuanheigu (LTH) and NILs IRBL4 (>80%), followed by IRBL1 and IRBL2 (>60%). Other NILs remained asymptomatic, as seen with the previous

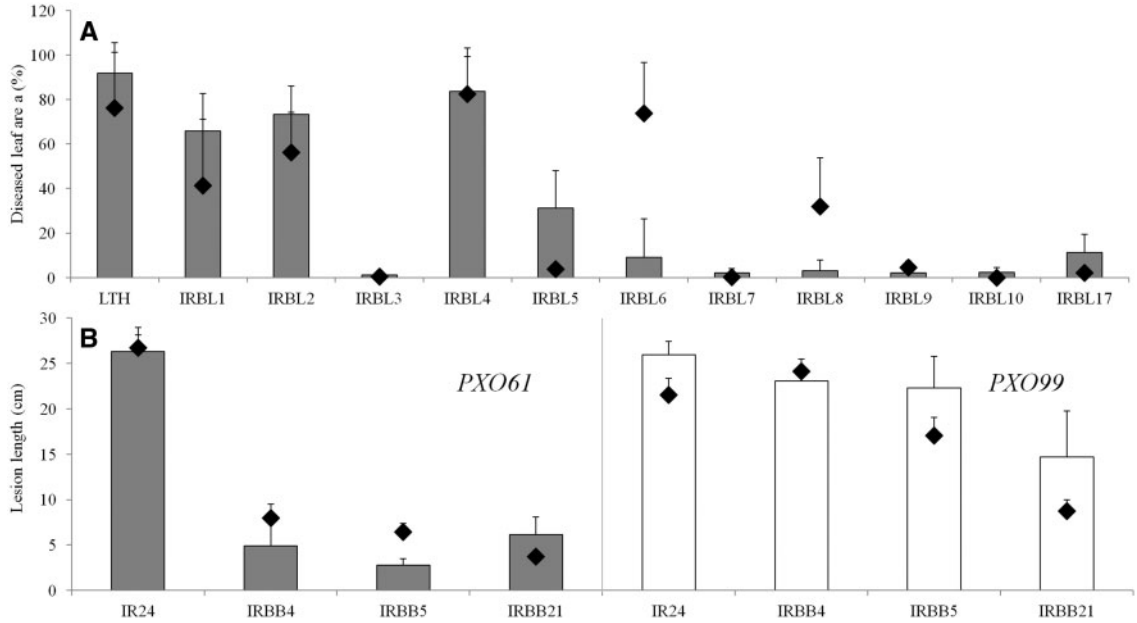

Fig. 1 Average values of 30 cycles of rice blast (grey columns, A) and six cycles of two bacterial blight strains: *PXO61* (grey columns, B) and *PXO99* (white columns, B), with respective values of the experimental season 2013 (black diamonds) for both the rice blast and bacterial blight experiment. (A) Diseased leaf area (%) at 15 DAI; (B) lesion length (cm) at 5 DAI for selected near-isogenic lines in the genetic background of susceptible cultivars LTH and IR24 ± SD, respectively.

30 cycles. In contrast to the screening of the previous 30 cycles, NIL IRBL5 expressed a smaller diseased leaf area, while IRBL6 and IRBL8 expressed a greater diseased leaf area during the wet season in 2013, indicating partial seasonal influence on the disease severity and spread.

Compared with RB, strong positive correlation ($R^2 = 0.85$, $P < 0.01$) between the previous six BB cycles and experimental results obtained during this study suggested low variation in the results, i.e. low seasonal and/or climatic influence on BB tested under greenhouse conditions. The highest lesion length at 5 DAI (~25 cm, **Fig. 1B**) was found in the case of the susceptible background IR24 for both BB strains (*PXO61* and *PXO99*). In principle, monogenic lines treated with the *PXO61* strain remained asymptomatic, with an approximate lesion length of ≤5 cm. Leaves treated with the more severe *PXO99* strain resulted in a lesion length varying from 15 cm (IRBB21) to 25 cm (IRBB4 and IRBB5).

To ascertain the impact of both RB and BB infection on rice cultivars known for their contrasting response to drought stress, the same conditions as mentioned above were imposed; the responses are presented in **Fig. 2**. The photographic view of the representative plants inoculated by RB (15 DAI; **Fig. 2A**) and spread of BB infection throughout the inoculated leaf (**Fig. 2B**) used during classical method for severity screenings. Compared with its RB resistance (no visible symptoms, **Fig. 2A, C**), cultivar N22 expressed the highest sensitivity to both BB strains, with lesion length of around 23 cm at 5 DAI (**Fig. 2D**). Cultivars highly (IR64) and moderately (NSIC Rc 222) sensitive to RB (diseased leaf area 32% and 6%, **Fig. 2C**) remained asymptomatic while exposed to *PXO61*; the BB strain, however, showed higher sensitivity to the *PXO99* strain (**Fig. 2D**).

Optical measurements

Chl-F imaging of RB and BB. Since Chl-F originates almost exclusively from the Chl *a* molecules located in the PSII complexes, concentrations of Chl *a* for NILs and the parents involved in the RB experiment (control and infected leaf tissue) are presented in Supplementary Fig. S1. Chl-F imaging was inspected for the RB and BB experiment, at pre-defined time intervals [non-destructive measurements (NDMs); see the Materials and Methods]. Subsequently, Chl-F parameters (Fv/F_M, QY and Ft) were calculated and tested. Fv/F_M was found to be most effective to discriminate RB and BB in all NILs under laboratory conditions (Figs. **3**, **4**). In agreement with conventional RB and BB visual screening, the first visible symptoms appeared at 8–9 DAI in the case of RB (Supplementary Fig. S2), and at 3 DAI in the case of BB (Supplementary Fig. S3). Since symptoms of both RB and BB were showing similar optical properties throughout the pathogen progress and time (Supplementary Figs. S2, S3), time points of 15 DAI for RB and 5 DAI for BB were selected for comparing plant–pathogen interactions in this study. **Fig. 3** shows representative images of the Fv/F_M parameter for 11 RB NILs; the left panel represents control (asymptomatic) leaves with Fv/F_M values around 0.83. This was lower in the case of visually non-infected parts surrounding the infected spots of these leaves (**Fig. 3**, right panel), with values ranging between 0.72 and 0.83 (**Fig. 4A**, red diamonds), for all inspected, pre-defined susceptible cultivars during 2013 (**Fig. 1A**; diamond symbols). Heterogeneous F_v/F_M distribution over all symptomatic leaves was characterized by a lower value in the infected spots of susceptible cultivars (**Fig. 4A**), with the highest decrease (0.5–0.55) expressed in IRBL8, IRBL1 and IRBL6. Similarly, NILs IRBL3, 7, 9, 10 and 17

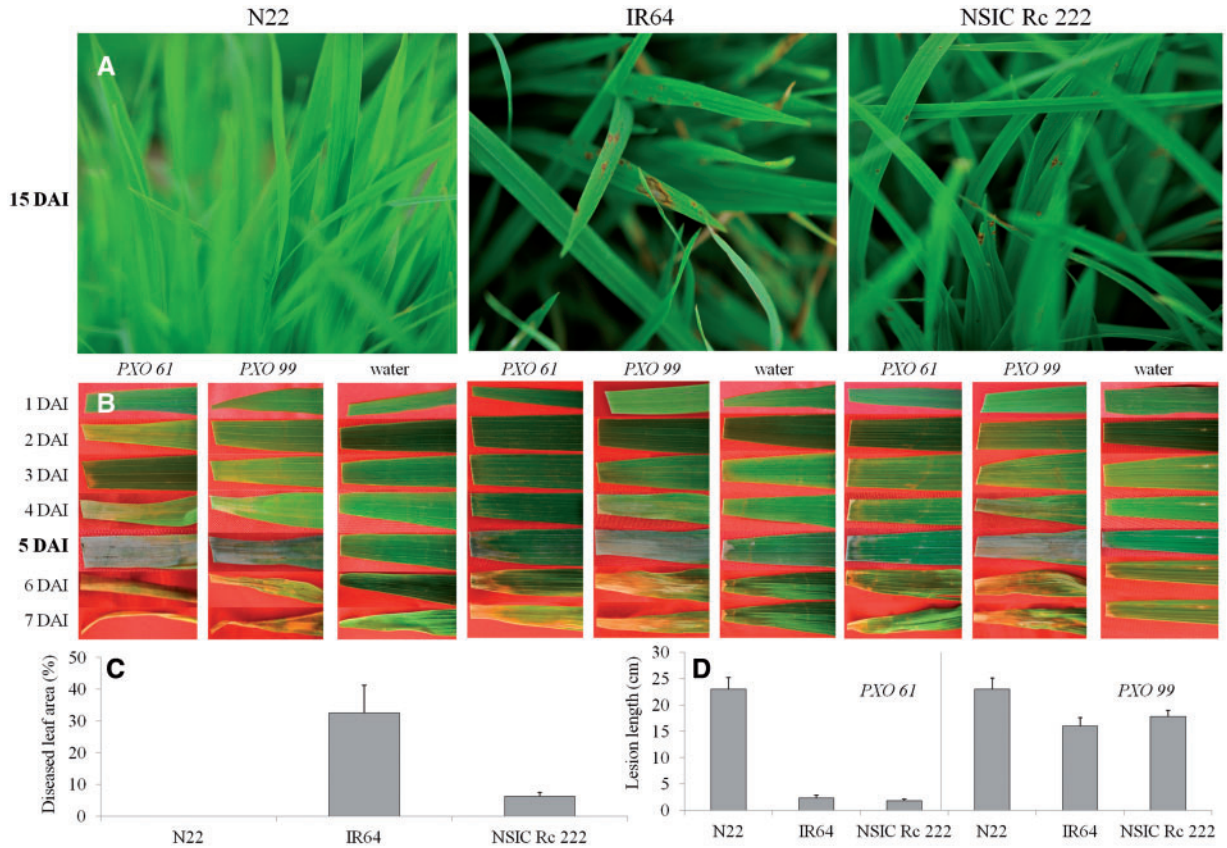

Fig. 2 Photographic view of rice blast (A), bacterial blight (B), and the representative values for classical severity screening of rice blast (C) and bacterial blight (D) for three cultivars known for their contrasting response to drought (N22, IR64 and NSIC Rc 222).

with the least infected area (**Fig. 1A**) also had the lowest or no reduction in Fv/F_M (**Fig. 4A**). By means of Chl-F imaging, BB spread of infection through the leaves was shown to result in a gradual decrease in Fv/F_M and was surrounded by leaf tissue expressing a higher physiological value for this parameter (Supplementary Fig. S3). The N22 cultivar expressed high sensitivity for both BB strains, while IR64 and NSIC Rc 222 were moderately resistant to *PXO61* and sensitive to *PXO99* BB strains (Supplementary Fig. S3).

By exposure of dark-adapted leaves to actinic light (see the Materials and Methods), (i) the level of the effective quantum yield of PSII in the light-adapted state (QY, **Fig. 4B**) and (ii) the approximate level of Chl-F in the steady state (Ft, **Fig. 4C**) were analyzed. As shown, both parameters exhibit similar patterns to those of the parameter Fv/F_M, while pre-defined sensitive NILs (**Fig. 1A**) were characterized by a lower value in infected leaf spots compared with the entire leaf area surrounding the infection. Similarly, no differences in resistant NILs were found for both the infected area and the entire leaf area. Irrespective of the analyzed parameter, a positive correlation between F_V/F_M and Ft ($R^2 = 0.65$, $P < 0.01$), and Fv/F_M and QY ($R^2 = 0.36$, $P < 0.01$) was recorded for all inspected rice cultivars.

Verification of selected Chl-F parameters under ambient light conditions. By applying Chl-F imaging technique, parameters suitable to detect both RB and BB were identified. For the field- and greenhouse-based phenotyping experiment, however, only the Chl-F parameters detectable under actual light conditions (QY and Ft) were inspected throughout the whole study, for the response to biotic and both biotic and abiotic stresses in selected rice cultivars.

For RB, the values of both parameters ranged from approximately 0.48 to 0.64 in the case of QY (**Fig. 5A**), and approximately >10,000 to 15,000 in the case of Ft for the control category (**Fig. 5C**), for resistant and/or sensitive cultivars shown in **Fig. 1A**. The QY tended to decrease with the impact of RB in the infected leaf spots (**Fig. 5A**) of susceptible NILs (IRBL2, 4, 5 and 6, but not IRBL1) compared with the surrounding entire leaf area, while the resistant NILs (IRBL3, 7, 9, 10 and 17) had a tendency to retain higher levels of QY. The lowest QY in infected leaf spots (0.36) was expressed by highly sensitive IRBL6. Also, a lower value of QY for control leaves compared with the entire leaf area was found in some cases. Noticeably, these values for the control were lower (~0.48–0.57) compared with the rest of the NILs. The lowest value of Ft (**Fig. 5C**, approximately 4,000 relative units) in the infected spots was expressed in sensitive NILs (IRBL4, IRBL6 and IRBL8), with the highest value (~8,500 relative units) expressed by two resistant NILs IRBL10 and IRBL17. In all investigated sensitive NILs, the area surrounding the infected leaf spots expressed a higher Ft value. In contrast to QY, pre-defined resistant NILs (**Fig. 1A**) expressed a pattern similar to those of sensitive NILs,

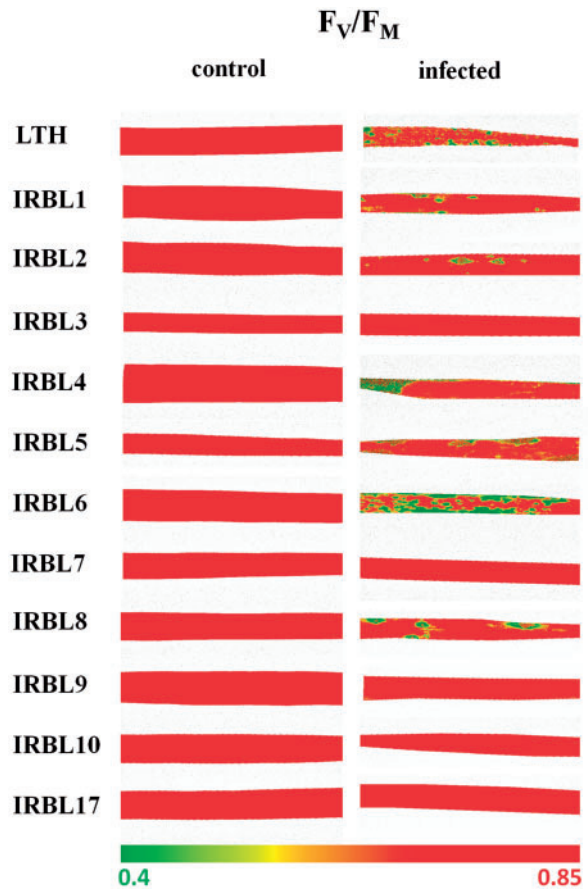

Fig. 3 False color scale images of maximum quantum yield of PSII (Fv/F_M). Distribution of the selected parameter over representative healthy leaves (control, left panel) and leaves infected by rice blast (infected, right panel) in near-isogenic lines in the genetic background of the susceptible cultivar LTH, measured at 15 DAI. Fv/F_M was measured in vivo, after dark adaptation of the sample for 20 min, in laboratory conditions. The color scale with minimum and maximum values is represented by the interval (0.40, 0.85).

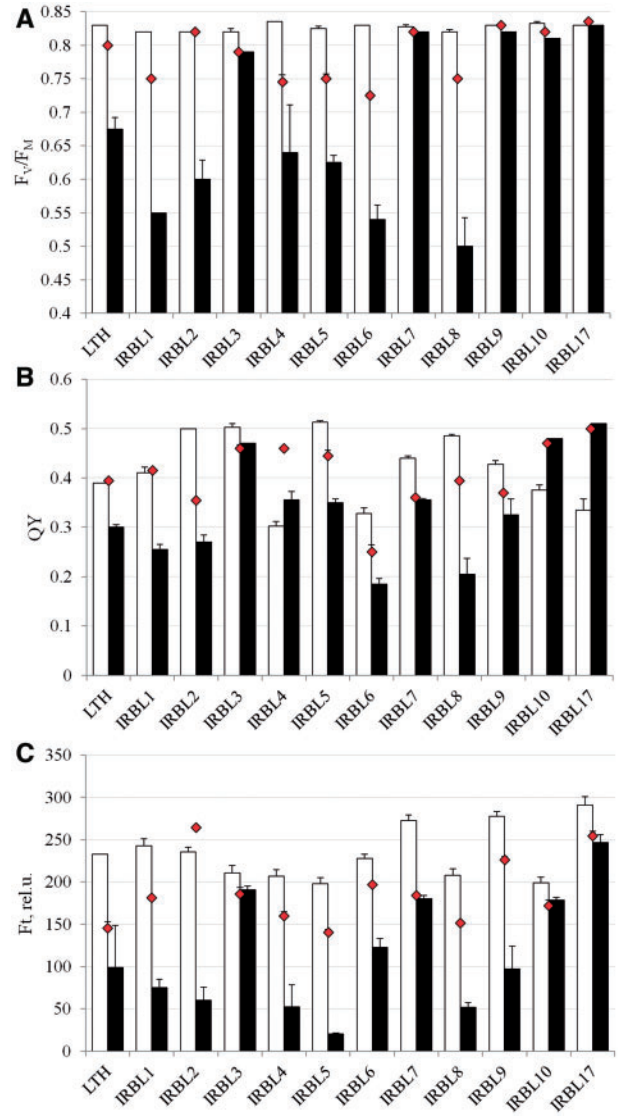

Fig. 4 Mean values of the maximum quantum yield of PSII (Fv/F_M, A), effective quantum yield of PSII (QY, B) and steady-state fluorescence level (Ft, C) after exposure to actinic light [~800 µmol (photons) m^{-2} s^{-1}] for 120 s, measured in laboratory conditions. Values represent control leaves (white columns), infected spots (black columns) and leaf tissue surrounding infected leaf spots (red diamonds) for 11 near-isogenic lines in the genetic background of the susceptible cultivar LTH measured at 15 DAI. Each data point represents the average of three points in a representative leaf ± SEM.

with Ft having similar expression patterns under stress, thus not allowing a clear differentiation between sensitive and tolerant NILs (**Fig. 5C**). A higher value of Ft in control leaf tissue was found in all inspected sensitive as well as resistant NILs (**Fig. 5C**).

Compared with RB, BB infection behaved differently. As shown in the photograph in **Fig. 2B**, the infection was characterized as a spread from the top of the leaf towards the entire leaf area and, thus, an alternative approach has been used to measure the impact on a whole-leaf basis (see the Materials and Methods). The value of QY in NILs under control conditions (**Fig. 5B**) ranged from 0.4 (IRBB5) to 0.53 (IR24). The more severe *PXO99* strain (**Fig. 1B**) resulted in a QY of 0.05 (IR24) and a maximum of 0.4 (IBB4), while *PXO61* strains expressed a comparably higher value, indicating lower severity of this strain (**Fig. 5B**). A similar observation was found in the case of Ft, where the more severe *PXO99* strain (**Fig. 5D**) resulted in a decrease of this parameter only in IR24 and IRBB5. With *PXO61*, both the parameters showed higher values than the control, influenced by the experimental set-up and the rate of spread of infection.

Comparative response of biotic and abiotic stress—Chl-F parameters. Both Chl-F parameters remained unchanged for the N22 cultivar, but decreased with the impact of RB in IR64 and NSIC Rc 222 (Supplementary Fig. S4A, C). Clear discrimination of these two Chl-F parameters was found in the case of BB (Supplementary Fig. S4B, D), where a visible decrease was observed in the N22 cultivar (both *PXO61* and *PXO99* strains).

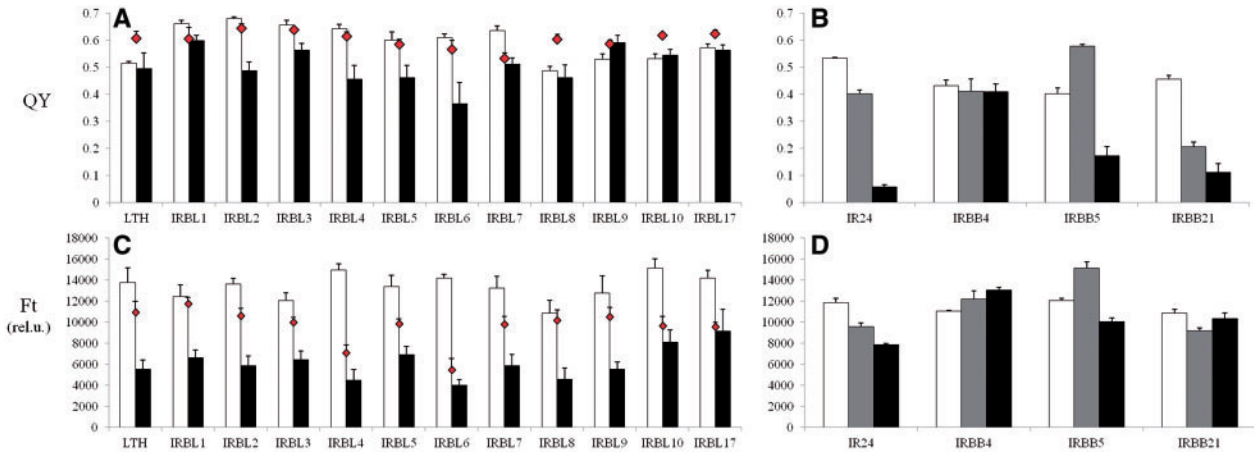

Fig. 5 Mean values of the effective quantum yield of PSII efficiency in the light-adapted state (QY, A, B) and the steady-state Chl-F level in the light-adapted state (Ft, C, D), measured in vivo under field (A, C) and greenhouse (B, D) conditions. Eleven near-isogenic lines in the genetic background of the susceptible cultivar LTH for rice blast and three representative near-isogenic lines in the genetic background of the susceptible cultivar IR24 for the bacterial blight experiment are represented by (A, C) and (B, D), respectively. White columns represent controls for both biotic stresses; for rice blast, black columns represent infected leaf spots and red diamonds represent the entire leaf area surrounding the spots where the infection started to propagate. For bacterial blight, gray and black columns represent strains *PXO61* and *PXO99*, respectively. Each data point represents the mean ± SEM. Note: for IRBB4 (B), the major portion of the leaf designated for stress measurements turned necrotic due to its extreme sensitivity, and the measurements presented are from the non-necrotic portion towards the base of the leaf, unlike others where measurements were taken from the mid portion of the leaf.

In contrast, IR64 and NSIC Rc 222 were not affected by *PXO61* strains, except for Ft which was reduced in NSIC Rc 222, while the impact of the severe *PXO99* strain was characterized by a higher decrease in QY compared with Ft. Similarly, several changes were visible for both parameters with drought stress exposure (Supplementary Fig. S5). For visualization, the significance of the differences between control and leaf tissue exposed to the stress (RB, BB and drought) is plotted in **Fig. 6**. Under drought stress, the values for both parameters differed significantly in the case of the NSIC Rc 222 cultivar for both T2 and T3 treatment. A different trend was observed in cultivar N22, where QY values were significantly lowered (T2, T3 and T4 treatments) which was, however, not captured by Ft (**Fig. 6**). A different response was recorded in T4 treatment with the IR64 cultivar; however, other treatments behaved similarly, with the same probability levels for both Chl-F parameters.

Comparative response of biotic and abiotic stress—reflectance measurements. Changes of spectral properties of the leaves for selected rice cultivars (N22, IR64 and NSIC Rc 222), under both biotic and abiotic stresses were investigated. Selected Vis (**Table 1**) were calculated and their applicability (the same approach as in the case of Chl-F parameters, i.e. comparison with classical severity screenings; **Fig. 2C, D**) were investigated. The N22 cultivar, resistant to RB (**Fig. 2C**) and highly sensitive to both BB strains (**Fig. 2D**), retained mostly non-significant differences in the case of RB (**Fig. 6**). In several cases (while comparing control and visibly healthy leaf tissue around the infected leaf spots), however, the value differed significantly (**Fig. 6**). While comparing the response of N22 to both BB strains, calculated Vis referred rather to the sensitivity of this cultivar. In a few cases (Vis designed for detection of RB and/or total Chl content), values showed a non-significant difference. Cultivars sensitive to RB (IR64 and NSIC Rc 222, **Fig. 2C**) expressed mostly significant differences with a high probability level. Also in a few cases (related mostly to the total Chl content), the sensitivity of these cultivars to RB was not captured by particular calculated Vis. As shown in **Fig. 2D**, both IR64 and NSIC Rc 222 cultivars behave as resistant to *PXO61*, compared with their sensitivity to the more severe *PXO99* strain. These classical severity screenings were followed by determination of Vis in most cases, where the cultivars either did not differ (*PXO61*) or differ significantly (*PXO99*) with certain probability levels (**Fig. 6**), indicating their resistance/sensitivity to a particular BB strain.

With the impact of drought applied at certain phenological stages (**Fig. 7C, D**), all three cultivars (N22, IR64 and NSIC Rc 222) behaved differently as seen by visualization of probability levels shown in **Fig. 6**. NSIC Rc 222 showed a highly sensitive response to drought stress exposure during both phenological stages T2 and T3 (**Fig. 6**), with only a few cases (related to Chl *a* and total Chl content, see **Table 1**), where it showed a non-significant difference. By employing RB-related Vis (see **Table 1**), N22 and IR64 cultivars behaved differently in response to drought; N22 expressed resistance in all treatments, while IR64 susceptibility was recorded across three (T3, T4 and T5) of the four tested developmental stages (**Fig. 6**). A similar observation was made in the case of Vis related to Chl *a* and Chl *b* content but not with a few Vis related to total Chl content (**Fig. 6**; **Table 1**). In the context of Vis developed for estimating total Chl (**Table 1**), N22 was affected by drought stress applied in three stages (**Fig. 6**), while IR64 indicated resistance in developmental stages T2 and T3.

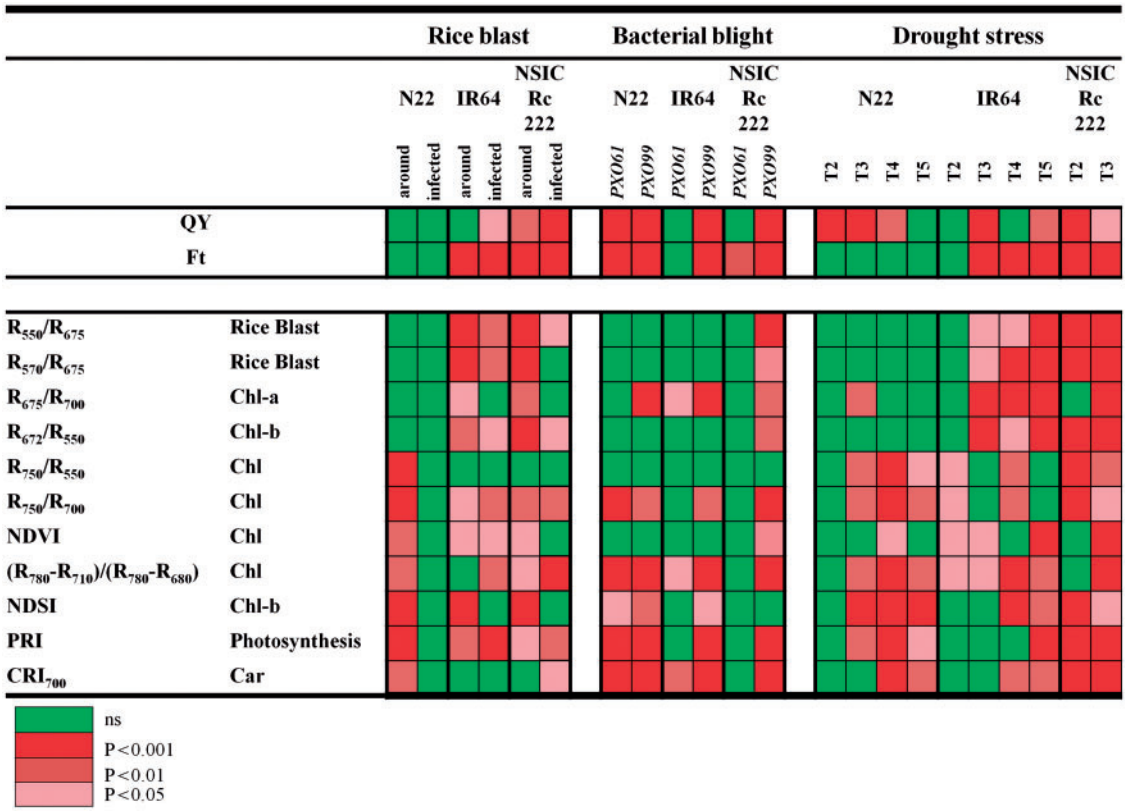

Fig. 6 Visualization of selected Chl-F parameters and vegetation indices, and their applicability to follow both biotic (rice blast, bacterial blight) and abiotic (drought) stresses. The significance of the difference between control and stressed leaf tissue for the representative rice cultivars [N22, IR 64 and NSIC Rc 222] is indicated by the color associated with the probability level in the key. For rice blast, 'around' denotes the significance between control and leaf tissue surrounding infected spots, while 'infected' denotes the significance between control and infected spots.

Table 1 Vegetation indices used in the study

Vis	Equation	Related to	Reference
RR	R_{550}/R_{675}	Rice blast	Kobayashi et al. (2003)
RR	R_{570}/R_{675}	Rice blast	Kobayashi et al. (2003)
RR	R_{675}/R_{700}	Chl *a*	Chapelle et al. (1992)
RR	R_{672}/R_{550}	Chl *b*	Datt (1998)
RR	R_{750}/R_{550}	Chl	Gitelson and Merzlyak (1994)
SRI	R_{750}/R_{700}	Chl	Gitelson et al. (1996)
NDVI	$(R_{755} + R_{664})/(R_{755} - R_{664})$	Chl	Rouse et al. (1974)
RR	$(R_{780} - R_{710})/(R_{780} - R_{680})$	Chl	Datt (1999)
NDSI	$(R_{550} - R_{410})/(R_{550} + R_{410})$	Chl *b*	Inoue et al. (2008)
PRI	$(R_{531} - R_{570})/(R_{531} + R_{570})$	Photosynthesis	Gamon et al. (1992)
CRI_{700}	$1/R_{510} - 1/R_{700}$	Car	Gitelson et al. (2002)

Car, total carotenoids; CRI_{700}, carotenoid reflectance index; NDSI, normalized difference spectral index; NDVI, normalized difference vegetation index; PRI, photochemical reflectance index; RR, reflectance ratio; SRI, structural reflectance index.

Discussion

The effects of fungal (RB) and/or bacterial (BB) pathogens on plant growth and survival are routinely evaluated by means of visual screening and rating methods. The major limitation of these methods, however, lies in the challenge of obtaining fast and accurate information about the plant/crop physiology and fitness. Both RB and BB would alter the distribution of light energy absorbed by Chl among the three mutually competing processes, i.e. photochemistry, thermal dissipation or Chl-F. Pathogen attack influences conformational changes in the PSII light-harvesting complexes and, thus, can lead to a shift

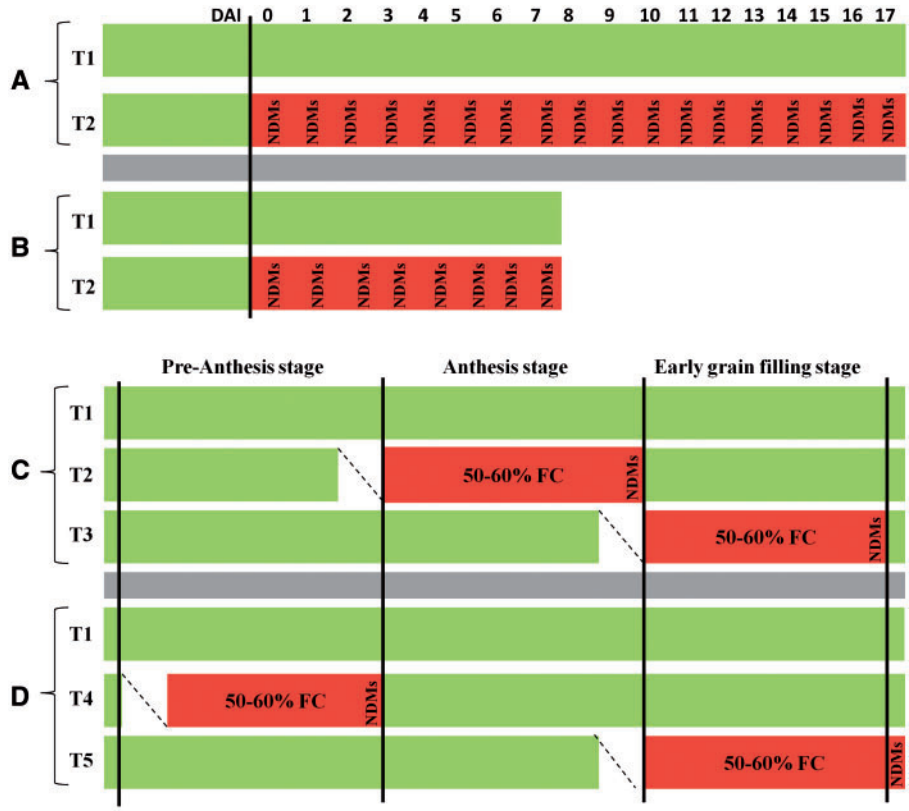

Fig. 7 Schematic view of non-destructive measurements (NDMs) for both biotic and abiotic experiments. Rice blast (A), bacterial blight (B) and two independent drought stress treatments (C, D), with T1 representing the control treatment for all experiments. For both biotic experiments, treatment (T2) represents days after inoculation (rice blast and bacterial blight, respectively) for biotic stresses. For two independent drought stress experiments (C, D), upper case 'T' indicates reduction in field capacity (FC) to 50–60% during: T2, anthesis; T3, early grain-filling stage; T4, pre-anthesis stage; and T5, early grain-filling stage until harvest.

in the share of these processes. Since, in infected plants, Chl-F would be the main dissipative process of excess energy, a Chl-F imaging system has been developed and broadly applied to visualize localized plant stress (reviewed by Nedbal and Whitmarsh 2004, Lenk et al. 2007). Despite the well-established approach of the combinatorial imaging technique presented by Berger et al. (2007), most often the values of various Chl-F parameters reflecting the physiological status of a plant are visualized and their applicability for stress detection is investigated. A similar approach to our study, i.e. analyzing several Chl-F parameters and subsequent selection of the best contrasting ones, has been used in a number of studies (e.g. Chaerle and Van der Straeten 2000). Depending on the level of resistance/susceptibility to both biotic stresses presented here, the physiology of plants was affected (Figs. **1**, **2**). Two standard Chl-F parameters [maximum and effective quantum yield of PSII; Fv/F_M (Kitajima and Butler 1975) and QY (Genty et al. 1989)] and one directly measured Chl-F parameter [steady-state Chl-F (Ft, Krause and Weis 1991)] met the above-mentioned requirements. As shown by Fv/F_M images (**Fig. 3**; Supplementary Figs. S2, S3), local perturbations in the photosynthetic efficiency of PSII were visible in both the spots (RB) and lesions (BB), which is in accordance with previously published results (Šebela et al. 2014). In our study, the standard value of Fv/F_M (~0.83; Bjorkman and Deming 1987) decreased with the onset of both RB and BB, where the appearance of visual symptoms was linked to the degradation of Chl resulting in discolored local infection spots or lesions. Throughout the leaves, pathogens influenced fluorescence characteristics either in the direct focus of infection or in the apparently healthy leaf areas surrounding the infection. These visually not infected parts expressed in some cases (**Fig. 4A**) lowered the physiological level of Fv/F_M compared with control leaves, indicating either damage in PSII reaction centers (susceptibility) or possible activation of the defense response and accumulation of resistance-specific compounds (tolerance). In the case of RB, the phenotypic response in the visually non-infected parts (**Fig. 4A**) differed even within the sensitive cultivars and/or progress of the different pathogens over time (Supplementary Fig. S2), but still followed the classical severity screenings (**Fig. 1A**). This observed discrepancy in photochemical efficiency of investigated NILs in the infection sites or the area surrounding the infection reflects different levels of sensitivity to a particular stress.

Compared with Fv/F_M, a major advantage of the other two identified parameters (QY and Ft) lies in the potential to be measured under natural conditions, without the need for dark adaptation (Rascher et al. 2000). The response of the parameter

QY in sensitive cultivars (**Fig. 4B**) indicates that photochemical energy conversion in PSII in infected spots or lesions was impaired. Moreover, in contrast to Fv/F_M (reporting mainly the injury of PSII complexes), QY and Ft also often report the yield of CO_2 fixation (Genty et al. 1989, Flexas et al. 2002), thus providing additional physiological information to quantify stress-induced damage in plants. Thus, in infected spots, reduction of these parameters reflects the decline in CO_2 fixation due to degradation of Chl. As shown in **Fig. 4**, QY varied (IRBL4, 10 and 17) as the controls were grown at a distant location (see the Materials and Methods), and hence were influenced by the sensitivity of Chl-F to other environmental factors. According to our expectation, these differences in control leaf tissue were neglibible while measuring the visibly non-infected portions of the leaf surrounding the area of infection in the stress plots.

Compared with RB, BB infection behaves differently. Fungal growth of RB builds up white to gray-green lesions or spots with a dark green border of mycelia occurring at the leaf surface (Babujee and Gnanamanickam 2000); BB develops a complex system of infection structures within the leaf structures. Gnanamanickam et al. (1999) suggested that BB produces tan-gray lesions along the veins, which was also seen in our study (**Fig. 2B**). Moreover, as shown in our study, the spread of these lesions differed among rice cultivars (Sonti 1998). Such diverse responses together with our experimental set-up for BB (the whole-leaf area basis; see the Materials and Methods) could explain the results obtained (for example, IRBB5, **Fig. 5**). NILs with more severe susceptibility to BB (e.g. IRBB4; **Fig. 1**) were not captured by Chl-F measurements, since half the leaf intended to be used for stress measurements was completely necrotic (**Fig. 5**). Such impairment of a fraction of energy converted in PSII reaction centers (followed by these Chl-F parameters) was captured in the case of three selected cultivars with differential drought response exposed to BB (N22, IR64 and NSIC Rc 222; Supplementary Fig. S4), as well as to RB, indicating less damage. The strength and usefulness of Ft for drought stress (Cerovic et al. 1996) has been proven by our experiment. As shown here, the drought stress-tolerant cultivar N22 expressed lower QY as a response to drought in the tested developmental stages (Supplementary Fig. S5; **Fig. 6**). With the more severe response of the sensitive varieties (IR64 and NSIC Rc 222) this disadvantage is negligible (i.e. excluding the necrotic leaf), which could potentially be the result of a more severe decrease of Chl and damage of PSII reaction centers. Hence, due to the extreme susceptibility of IRBB4 for both strains of BB (**Fig. 5**) and for drought stress exposure in IR64 and NSIC Rc 222 (Supplementary Fig. S5), a major portion of the target leaf turned necrotic and the data presented in these figures are from a non-necrotic portion of the same leaf towards the base of the leaf.

Similar to our study (Supplementary Fig. S1), a partial decrease of Chl *a* was previously reported with the impact of RB (Bastiaans and Roumen 1993). This decrease can be caused by the breakdown of the Chl molecule, inhibition of Chl synthesis or a reduction in the number of chloroplasts which influences the reflectance spectrum of the leaves (Blackburn 2007). As expected, during pathogen-activated Chl breakdown which results in the fading of the green color in infected spots or lesions, the percentage increase of reflected light is higher for the blue and red (maximum absorptivity of Chl) compared with the green (minimum absorptivity of Chl) spectrum of light. In our study, we proved that Vis designed for RB detection were the most effective to follow RB disease severity (**Fig. 6**). These Vis are calculated from wavelengths of both the sensitivity maxima and minima to this fungal infection (Carter 1991, Kobayashi et al. 2001). It can also explain the high accuracy of Chl *b*-related Vis combining both sensitivity maxima and minima (Datt 1998), and, on the other hand, low accuracy of Chl *a* Vis calculated just from wavelengths belonging to the region of sensitivity minima (Chapelle et al. 1992). All selected total Chl-related Vis calculated in our study used off-Chl absorption center wavebands, influenced mainly by leaf structure, anatomy or water content, rather than by Chl content (Devi and Sharama 2010). As shown in **Fig. 6**, these Vis together with those related to photosynthetic performances [photochemical reflectance index (PRI)] and/or carotenoid content (CRI_{700}) behaved differently when comparing controls and leaf tissue around the infection of stressed N22, possibly due to their sensitivity to the changes caused by environmental or management practice (e.g. different fertilizer combinations), and/or environmental effect of true controls cultivated at a distance (see the Materials and Methods). Changes of Chl concentrations (Supplementary Fig. S1B) on exposure to RB in sensitive rice cultivars (**Fig. 2A, C**) followed Chl-related Vis (**Fig. 6**), generated using the minimal sensitivity (Kobayashi et al. 2003) in combination with the maximal sensitivity wavelength (Gitelson et al. 1996). However, the same was not captured when specific wavelengths belonging only to sensitivity maxima [i.e. green (Gitelson and Merzlyak 1994), (R_{510} and R_{570}, Gitelson et al. 2002)], minima [red (R_{664}, Rouse et al. 1974)] and/or ICCW (in-chlorophyll centre waveband, Datt 1999) were implemented. According to the literature (Yang 2010), the most effective Vis to detect BB were those calculated from NIR with zero influence of Chl (**Fig. 6**). Also, failure of Vis calculated from maximal (green) and minimal (red) sensitivity wavelengths could explain the morphological and anatomical changes of the leaves rather than direct Chl concentration changes due to BB.

Despite the known relationship between water content of the plant and NIR-based Vis (Penuelas et al. 1997, Ceccato et al. 2001), both the visible- and NIR-related Vis (**Table 1**) were calculated. A common observation in this study was that the Vis using a combination of ICCW and/or the green spectrum of reflected light were able to differentiate resistant (N22) from sensitive (IR64) cultivars. This supported the observations documenting heat tolerance of N22 during the reproductive stage (Jagadish et al. 2010) and/or a combination of heat/drought tolerance (Liu et al. 2006, Rang et al. 2011). On the basis of Vis related to Chl detection at these wavelengths, the resistant cultivar N22 did not differ compared with the sensitive cultivar IR64. Also NSIC Rc 222 reduced its Chl content under the impact of drought stress. In contrast, a common feature for selected Vis calculated from off-Chl absorption center wavebands, influenced rather by changes in leaf structure

(Knipling 1970) or leaf anatomy/water content, did not differentiate resistant from sensitive cultivars (Fig. 6). This observation can be explained with irreversible changes in the anatomy of flag leaves playing a decisive role in acquiring drought tolerance (Zagdanska and Kozdoj 1994). Such changes allow the plant to conserve internal water content under the impact of drought stress developed in a resistant cultivar (N22), and/or the consequence of internal water loss in the case of sensitive cultivars (IR64 and NSIC Rc 222).

In summary, the non-invasive Chl-F and reflectance-based analysis of rice response under both biotic and abiotic stress impact presented here strengthens existing physiological studies. Approaches presented, together with the classical severity screenings, allowed the accurate quantification of both biotic (RB and BB) and abiotic stresses. Moreover, the use of the techniques presented minimizes the time needed for stress detection, thus allowing field phenotyping of a large set of cultivars for capturing unexplored genetic diversity for stress resilience. Additionally, the techniques presented, with minor modifications, can be used for quantifying other biotic and abiotic stresses such as salinity, as the impact of these stresses affects the PSII as demonstrated above. Apart from the usefulness of other Vis presented here, the PRI index emerged as a good alternative to Chl-F. These findings, while applied at the canopy level, in the combination of different approaches investigated by the authors (e.g. 3D Chl-F and/or UV-induced fluorescence and/or reflectance during biotic stresses) reveals significant improvement in phenotyping for enhancing the capacity of ongoing rice biotic and abiotic stress breeding programs.

Materials and Methods

Both the field (RB) and the greenhouse (BB and drought stress) experiments were conducted at the International Rice Research Institute (IRRI), Los Baños Laguna, Philippines (14°11′N, 121°15′E), during the wet season 2013.

Plant material

Biotic stress experiments. For the field experiment with RB, the susceptible cultivar (LTH) and a series of monogenic lines with a varying level of tolerance/susceptibility to RB (see Table 2) in the LTH background, and rice cultivars known for their contrasting response to drought stress [N22 (highly tolerant), IR64 (highly susceptible, see Liu et al. 2006, Jagadish et al. 2010, Rang et al. 2011) and NSIC Rc 222 (a popular variety in the Philippines whose response to drought stress is not known)] were cultivated in the IRRI blast nursery (Supplementary Fig. S6), where natural blast infection was highly favorable. As RB populations are very diverse, it is essential that the cultivars are evaluated in reponse to a wide range of pathogen populations. To maintain a high pathogen population (natural source of inoculum) in the blast nursery, eight rice cultivars with varying levels of susceptibility to RB were continuously planted at the site to provide a source of inoculum for experimental purposes (Kobayashi et al. 2007). The dormancy of the seeds (LTH, monogenic lines and the contrasting drought stress response cultivars) was broken by exposing them to 50°C for 3 d; pre-germinated seeds were sown and plants were cultivated under natural conditions, from June to July 2013. Evaluation for RB disease response was carried out between 0 and 17 d after exposure to the inoculum (Fig. 7A), with 0 indicating the day of inoculation. Assessment for blast severity was based on the percentage diseased leaf area. In order to ensure that control plants were well protected from any blast infections, a large tray (5 × 1.5 × 0.3 m) filled with the same soil was used to grow the entire set of lines at a similar density, at a far off location, from July to August 2013. Since the experimental set-up did not allow fluorescence images to be taken in the field conditions, leaves were not tagged and individual observations were recorded randomly, on three selected and detached plants (see further for additional details), at each measuring time point.

For the greenhouse experiment with BB, rice cultivars (IR24, IRBB4, IRBB5 and IRBB21; Table 2) and the same set of contrasting drought stress-responsive cultivars used in the RB experiment (N22, IR64 and NSIC Rc 222) were cultivated under greenhouse conditions. The dormancy of the seeds was also broken as mentioned above, and pre-germinated seeds were sown directly in pots (22 × 11 × 8.2 cm) filled with clay loam soil. Plants were cultivated from July to September 2013. Plants were grown until 45–55 d after sowing (maximum tillering stage) and inoculated with different *Xoo* races by the clipping method (Kauffman et al. 1973). Briefly, approximatley 1–2 cm of the leaf tip was cut with a pair of scissors dipped in bacterial suspension, at a concentration of 10^8–10^9 bacterial cells ml^{-1}. An equal number of plants were managed at a sufficient spatial distance with a physical barrier to avoid any contamination due to inoculum drift. The same procedure was followed with scissors dipped in distilled water to represent true controls. For each treatment, three flag leaves were selected and tagged; Chl-F and reflectance measurements were recorded on this set of leaves throughout the whole experiment (Fig. 7B).

For drought stress experiments in the greenhouse, rice cultivars known for their drought responsiveness at the critical flowering stage (N22 and IR64) and a popular variety NSIC Rc 222 (the same set of cultivars included in RB and BB experiments) were used to compare responses across both biotic and abiotic stresses. Similar to both the biotic experiments, the dormancy of the seeds was broken, and pre-germinated seeds were sown directly into pots (55 cm long, 15 cm diameter), filled with 11 kg of clay loam soil and maintained under natural greenhouse conditions at IRRI. The pots had holes on either sides at the bottom to allow for draining water, to impose controlled drought stress and to reach the desired levels of stress at the targeted stages (Fig. 7C, D). Plants were maintained under two moisture regimes, i.e. non-stressed or control at 100% field capacity (FC) and drought stress at 50–60% FC imposed during: (i) two targeted stages, i.e. at anthesis (T2) and the early grain-filling stage (T3) in one experiment involving all the three cultivars (Fig. 7C); and at (ii) pre-anthesis (T4) and the early grain-filling stage (T5) in another independent experiment involving just N22 and IR64 (Fig. 7D). Drought stress was imposed following a gravimetric approach (Kadam et al. 2015) and maintained at this level until coinciding with the target developmental stages. For each treatment, two flag leaves were selected, tagged and inspected.

Optical measurements

Non-destructive optical measurements (NDMs; Chl-F and reflectance) from both biotic and abiotic experiments were recorded at pre-defined time intervals (Fig. 7). Specifics of the measurements are detailed below.

Validation of Chl-F imaging procedure. Hypothesizing potential problems associated with detaching rice leaves from the plant followed by dark adaptation under laboratory conditions during the RB experiment, we have investigated a series of scenarios related to the status of the detached leaf or the storage procedure and resulting leaf rolling and/or fluorescence signal, respectively. Five scenarios were tested on representative leaves from cultivar N22, i.e. (i) detached leaves; (ii) detached leaves with the petiole coated with wet cellulose; (iii) the whole seedling uprooted along with the roots and its leaves used for measurements; (iv) similar to (iii) but roots were coated with wet cellulose; and (v) leaves chosen from plants cultivated in pots without any physical damage. To prove the reproducibility and reliability of the results, two leaves for each of the above five scenarios were dark adapted for 20 min, followed by measurements of the maximum quantum yield of PSII photochemistry (Fv/F_M; Kitajima and Butler 1975). Rolling of the leaves appeared in all five investigated scenarios; however, in scenarios (iv) and (v) optical measurements were not affected. The expected value of Fv/F_M (~0.83) was observed in the scenario with plants measured directly in pots (v) and similarly with (iv) whole seedlings detached with the roots coated with wet cellulose (data not shown). Other inspected categories expressed either rolling or reduced Fv/F_M values, indicating stress induction and, hence, all further Chl-F induction kinetics measurements were recorded from uprooted seedlings with roots coated with wet cellulose.

Table 2 Overview of monogenic lines with individual rice blast resistance Pi genes in the genetic background of the susceptible cultivar LTH and individual bacterial blight resistance Xa genes in the genetic background of the susceptible cultivar IR24 used in rice blast and bacterial blight experiments, respectively

Lines	Designation	Gene	Chromosome	Reference
Rice blast				
LTH	Lijiangxintuanheigu			
IRBL1	IRBLa-A	Pia	7	Yi et al. (2004)
IRBL2	IRBLa-C	Pia	7	Yi et al. (2004)
IRBL3	IRBLi-F5	Pii	9	Jeon et al. (2003)
IRBL4	IRBLks-F5	Pik-s	11	Luo et al. (2002)
IRBL5	IRBLks-S	Pik-s	11	Luo et al. (2002)
IRBL6	IRBLk-ka	Pik	11	Hayashi et al. (2006)
IRBL7	IRBLkp-60	Pik-p	11	Hayashi et al. (2006)
IRBL8	IRBLkh-K3	Pik-h	11	Fjellstrom et al. (2004)
IRBL9	IRBLz-Fu	Piz	6	Hayashi et al. (2006)
IRBL10	IRBLz5-CA	Piz5	6	Zhou et al. (2006)
IRBL17	IRBLsh-B	Pish	11	Hayashi et al. (2006)
Bacterial blight				
IR24		Xa18		
IRBB4		Xa4	11	Sun et al. (2003)
IRBB5		Xa5	5	Blair et al. (2003)
IRBB21		Xa21	11	Song et al. (1995)

Chl fluorescence and reflectance signals for stress phenotyping in rice

Kinetic imaging of Chl-F. Chl-F induction kinetics in both biotic experiments (RB and BB) were measured by a commercial kinetic imaging fluorometer (Handy FluorCam FC 1000, Photon System Instruments, Ltd.) under laboratory conditions. For each measuring date (**Fig. 7A, B**), a representative leaf of the plant (RB) and/or a tagged leaf (BB) was selected. The minimum fluorescence yield (F_0) was measured after 20 min dark adaptation, by applying short, low intensity measuring flashes [$\lambda_{max} \approx 620$ nm, approximately 3 μmol (photons) m^{-2} s^{-1}]. A short saturating pulse [1 s, white light, intensity approxinately 3,000 μmol (photons) m^{-2} s^{-1}] was applied to measure maximum Chl-F in the dark (F_M). The maximum quantum yield of PSII photochemistry (Fv/F_M; Kitajima and Butler 1975) was then calculated by using the following formula: $Fv/F_M = (F_M - F_0)/F_M$. After 17 s of dark relaxation, the sample was exposed to continuous actinic light illumination [70 s, 600 μmol (photons) m^{-2} s^{-1}] to reach the approximate level of Chl-F in the steady state (Ft; Schreiber et al. 1986). It was defined as the Chl-F intensity at the end of the actinic light period, after which a saturating pulse [1 s, white light, approximately 3,000 μmol (photons) m^{-2} s^{-1}] was applied to measure the steady-state maximum fluorescence in the light-adapted state (F_M'). Quantum yield of PSII in the light-adapted state (QY; Genty et al. 1989) was then calculated according to the formula: $(F_M' - F_t)/F_M'$. Transients were recorded by CCD camera in a series of 512 × 512 pixel images, with 12-bit resolution. Images of three selected conventional Chl-F parameters (Fv/F_M, QY and Ft) were analyzed to assess whether they displayed differences between control and stressed leaf tissue. Images of Chl-F were taken from a representative leaf of each cultivar in the case of RB and BB (**Table 2**), at 0–17 DAI (RB, **Fig. 7A**) and at 0–7 DAI (BB, **Fig. 7B**), respectively. For the cultivars contrasting in drought stress response exposed to biotic stresses, images were taken just for BB, in the case of both control and infected leaf tissue.

Chl-F parameters. The Chl-F measurements involving both biotic and abiotic experiments under field (RB) and greenhouse (BB and drought) conditions were performed using a portable fluorometer (FluorPen FP 100, Photon System Instruments, Ltd.; Supplementary Fig. S7). Saturating light [intensity approximately 3,000 μmol (photons) m^{-2} s^{-1}] and measuring light [intensity approximately 0.09 μmol (photons) m^{-2} s^{-1}] were applied to measure the effective quantum yield of PSII in the light-adapted state (QY; Genty et al. 1989) and the continuous fluorescence yield in the light-adapted state (Ft; Krause and Weis 1991). In total, nine replicate measurements were recorded in the case of RB at the time points (recorded temporally from 0 to 17 DAI) shown in **Fig. 7A** for control, selected infected leaf spots and leaf tissue area surrounding the leaf spots (three measurements each per three leaves). The same number of measurements was recorded throughout the whole leaf for control and/or throughout the whole leaf area including both infected and visibly healthy leaf tissue for both BB strains at the time points indicated in **Fig. 7B**. In the case of drought stress, three measurements per leaf (in total six replicate measurements) from selected control and stressed leaf tissue throughout the representative leaves were measured at the time points indicated in **Fig. 7C** and **D**.

Reflectance measurements. All field (RB) and greenhouse (BB and drought) measurements were performed by using the prototype of the hand-held instrument WinePen (Photon System Instruments, Ltd.; Supplementary Fig. S7), capable of measuring reflectance in the spectral range 325–780 nm. An incandescent xenon lamp was used as a light source, while the signal was detected by a compact polychromator integrated with a reflection grating and CMOS linear image sensor with the spectral response half-width of 9 nm and wavelength reproducibility of ±0.5 nm. For the instrument calibration, zenith standards were used. Several Vis, which have been reported in the literature and proven to be well correlated with abiotic stress in rice and/or with photosynthetic pigment concentration across the species (**Table 1**), were selected and calculated to standardize the application of reflectance measurements in quantifying the impact of both biotic and abiotic stresses. Namely, specific wavelengths of sensitivity maxima (green region: R_{550} and R_{570}), minima (specific in the Chl center waveband range ICCW; red region: $R_{640-680}$) and zero off-Chl absorption (NIR region) were used to calculate selected Vis.

Chemical analysis

Two fresh leaves from each monogenic line and each representative rice cultivar (N22, IR64 and NSIC Rc 222) used in the RB experiment (**Table 2**) were sampled. Leaves were collected at different time points, i.e. every third day beginning with the first DAI for stress treatment; and the first, seventh and 15th DAI for control treatments. Samples were frozen in liquid N and stored at −80°C until further use. Approximately 10 mg of freeze-dried sample was then

homogenized, sprinkled with 100 µl of distilled water, and extracted in 10 ml of 80% ethanol. Homogenate was incubated in test tubes wrapped in aluminum foil and left overnight at room temperature without disturbance. Pigments were determined spectroscopically, by detecting absorption spectra at specific wavelengths using a spectrophotometer (Schimadzu UV-1800). Chl *a* concentration was then calculated according to Lichtenthaler (1987) and expressed on a fresh weight basis.

Data analysis

Image analysis was performed using software FluorCam 7 (Photon System Instruments, Ltd.); significance and regression analysis were determined by using MS Excel.

Supplementary data

Supplementary data are available at PCP online.

Funding

This work was supported by The Federal Ministry for Economic Cooperation and Development, Germany; the Research Infrastructure project EPPN [FP7; Grant Agreement No. 284443]; and the Ministry of Education, Youth and Sports, Czech Republic [grant Nos. LO1415 and LM2015061].

Disclosures

The authors have no conflicts of interest to declare.

References

Babujee, L. and Gnanamanickam, S.S. (2000) Molecular tools for characterization of rice blast pathogen (*Magnaporthe grisea*) population and molecular marker-assisted breeding for disease resistance. *Curr. Sci.* 78: 248–257.

Bastiaans, L. (1991) Ratio between virtual and visual lesion size as a measure to describe reduction in leaf photosynthesis of rice due to leaf blast. *Phytopathology* 81: 611–615.

Bastiaans, L. and Roumen, E.C. (1993) Effect on leaf photosynthetic rate by leaf blast for rice cultivars with different types and levels of resistance. *Euphytica* 66: 81–87.

Berger, S., Benediktyová, Z., Matouš, K., Bonfig, K., Mueller, M.J., Nedbal, L., et al. (2007) Visualization of dynamics of plant–pathogen interaction by novel combination of chlorophyll fluorescence imaging and statistical analysis: differential effects of virulent and avirulent strains of *P. syringae and of oxylipins on A. thaliana. J. Exp. Bot.* 4: 797–806.

Bjorkman, O. and Demming, B. (1987) Photon yield of O_2 evolution and chlorophyll fluorescence characteristics at 77K among vascular plants of diverse origins. *Planta* 170: 489–504.

Blackburn, G.A. (2007) Hyperspectral remote sensing of plant pigments. *J. Exp. Bot.* 58: 855–867.

Blair, M.W., Garris, A.J., Iyer, A.S., Chapman, B., Kresowich, S. and Mc Couch, S.R. (2003) High resolution genetic mapping and candidate gene identification at the *Xa5* locus for bacterial blight resistance in rice (*Oryza sativa* L). *Theor. Appl. Genet.* 107: 62–73.

Carter, G.A. (1991) Primary and secondary effects of water content on the spectral reflectance of leaves. *Amer. J. Bot.* 78: 916–924.

Ceccato, P., Flasse, S., Tarantola, S., Jacquemond, S. and Grégoire, J.M. (2001) Detecting vegetation leaf water content using reflectance in the optical domain. *Remote Sens. Environ.* 77: 22–33.

Centritto, M., Lauteri, M., Monteverdi, M.C. and Serraj, R. (2009) Leaf gas exchange, carbon isotope discrimination, and grain yield in contrasting rice genotypes subjected to water deficits during the reproductive stage. *J. Exp. Bot.* 8: 2325–2339.

Cerovic, Z.G., Goulas, Y., Gorbunov, M., Briantais, J.M., Camenen, L. and Moya, I. (1996) Fluorosensing of water stress in plants: diurnal changes of the mean lifetime and yield of chlorophyll fluorescence, measured simultaneously and at distance with a $_{T}$-LIDAR and a modified PAM-fluorimeter, in maize, sugar beet and Kalanchoe. *Remote Sens. Environ.* 58: 311–321.

Chaerle, L. and Van Der Straeten, D. (2000) Imaging techniques and the early detection of plant stress. *Trends Plant Sci.* 5: 495–501.

Chapelle, E.W., Kim, M.S. and Mc Murtrey, J.E. (1992) Ratio analysis of reflectance spectra (RARS): an algorithm for the remote estimation of the concentrations of chlorophyll a, chlorophyll b and carotenoids in soybean leaves. *Remote Sens. Environ.* 39: 239–247.

Chu, Z., Fu, B., Yang, H., Xu, C., Li., Z., Sanchez, A., et al. (2006a) Targeting *xa13*, a recessive gene for bacterial blight resistance in rice. *Theor. Appl. Genet.* 112: 455–461.

Chu, Z., Yuang, M., Yao, J., Ge, X., Yuan, B., Xu, C., et al. (2006b) Promoter mutations of an essential gene for pollen development result in disease resistance in rice. *Genes Dev.* 20: 1250–1255.

Chutia, J. and Borah, P.S. (2012) Water stress effect on leaf growth and chlorophyll content but not the grain yield in traditional rice (*Oryza sativa* L.) genotypes of Asssam, India II. Protein and proline status in seedlings under PEG induced water stress. *Amer. J. Plant Sci.* 3: 971–980.

Cottyn, B. and Mew, T. (2004) Bacterial blight of rice. *In* Encyclopedia of Plant and Crop Science. Edited by Goodman, R.M. Taylor and Francis, Abingdon, UK.

Datt, B. (1998) Remote sensing of chlorophyll a, chlorophyll b, chlorophyll a+b and total carotenoid content in eucalyptus leaves. *Remote Sens. Environ.* 66: 111–121.

Datt, B. (1999) Visible/near infrared reflectance and chlorophyll content in eucalyptus leaves. *Int. J. Remote Sens.* 20: 2741–2759.

Devi, S. and Sharma, G.D. (2010) Blast disease of rice caused by *Magnaporthe grisea*: a review. *Assam Univ. J. Sci. Technol.* 6: 144–154.

Fiorani, F. and Schurr, U. (2013) Future scenarios for plant phenotyping. *Annu. Rev. Plant Biol.* 64: 267–291.

Fjellstrom, R., Conaway-Bormans, C.A., Mc Clung, A.M., Marchetti, M.A., Shank, A.R. and Park, W.D. (2004) Development of DNA markers suitable for marker assisted selection of three Pi genes conferring resistance to multiple *Pyricularia grisea* pathotypes. *Crop Sci.* 44: 1790–1798.

Flexas, J., Escalona, J.M., Evain, S., Gulías, J., Moya, I., Osmond, C.B., et al. (2002) Steady-state chlorophyll fluorescence (Fs) measurements as a tool to follow variations of net CO_2 assimilation and stomatal conductance during water-stress in C_3 plants. *Physiol. Plant.* 114: 231–240.

Gamon, J.A., Penuelas, J. and Field, C.B. (1992) A narrow-waveband spectral index that tracks diurnal changes in photosynthetic efficiency. *Remote Sens. Environ.* 41: 35–44.

Genty, B., Briantais, J.M. and Baker, N.R. (1989) The relationship between the quantum yield of photosynthetic electron transport and quenching of chlorophyll fluorescence. *Biochim. Biophys. Acta* 990: 87–92.

Gitelson, A.A. and Merzlyak, M.N. (1994) Spectral reflectance changes associated with autumn senescence of *Aesculus hyppocastanum* L. and *Acer platanoides* L. leaves. Spectral features and relation to chlorophyll estimation. *J. Plant Physiol.* 143: 286–292.

Gitelson, A.A., Merzlyak, M.N. and Lichtenthaler, H.K. (1996) Detection of red edge position and chlorophyll content by reflectance measurements near 700 nm. *J. Plant Physiol.* 148: 501–508.

Gitelson, A.A., Zur, Y., Chivkunova, O.B. and Merzlyak, M.N. (2002) Assessing carotenoid content in plant leaves with reflectance spectroscopy. *Photochem. Photobiol.* 75: 272–281.

Gnanamanickam, S.S., Priyadarisini, V.B., Narayanan, N.N., Vasudevan, P. and Kavitha, S. (1999) An overview of bacterial blight disease of rice and strategies for its management. *Curr. Sci.* 77: 1435–1443.

Gu, J., Yin, X., Stompth, T.J., Wang, H. and Struik, P.C. (2012) Physiological basis of genetic variation in leaf photosynthesis among rice (*Oryza sativa* L.) introgression lines under drought and well-watered conditions. *J. Exp. Bot.* 14: 5137–5153.

Hatch, M.D. and Slack, C.R. (1970) Photosynthetic CO_2—fixation pathways. *Annu. Rev. Plant Physiol.* 21: 141–162.

Hayashi, K., Yoshida, H. and Ashikawa, I. (2006) Development of PCR-based allele-specific and InDel marker sets for nine rice blast resistance genes. *Theor. Appl. Genet.* 113: 251–260.

Inoue, Y., Penuelas, J., Miyata, A. and Mano, M. (2008) Normalized difference spectral indices for estimating photosynthetic efficiency and capacity at a canopy scale derived from hyperspectral and CO_2 flux measurements in rice. *Remote Sens. Environ.* 112: 156–172.

IPCC (2013) Fifth Assessment Report Climate Change 2013: Summary for Policymakers. Cambridge University Press.

Jagadish, S.V.K, Muthurajan, R., Oane, R., Wheeler, T.R., Heuer, S., Bennett, J., et al. (2010) Physiological and proteomic approaches to address heat tolerance during anthesis in rice (*Oryza sativa* L.). *J. Exp. Bot.* 61: 143–156.

Jagadish, S.V.K., Septiningsih, E.M., Kohli, A., Thomson, M.J., Ye, C., Redoña, E., et al. (2012) Genetic advances in adapting rice to a rapidly changing climate. *J. Agron. Crop Sci.* 198: 360–373.

Jeon, J.S., Chen, D., Yi, G.H., Wang, G.L. and Ronald, P.C. (2003) Genetic and physical mapping of *Pi5(t)*, a locus associated with broad-spectrum resistance to rice blast. *Mol. Genet. Genomics* 269: 280–289.

Kadam, N.N., Yin, X., Bindraban, P.S., Struik, P.C. and Jagadish, S.V.K. (2015) Does morphological and anatomical plasticity during the vegetative stage make wheat more tolerant of water deficit stress than rice? *Plant Physiol.* 167: 1389–1401.

Kauffman, H.E., Reddy, A.P.K., Hsieh, S.P.Y. and Merca, S.D. (1973) An improved technique for evaluating resistance of rice varieties to *Xanthomonas oryzae*. *Plant Dis. Rep.* 57: 537–541.

Khush, G.S. (2005) What it will take to feed 5.0 billion rice consumers in 2030. *Plant Mol. Biol.* 59: 1–6.

Khush, G.S. and Angeles, E.R. (1999) A new gene for resistance to race 6 of bacterial blight in rice, *Oryza sativa* L. *Rice Genet. Newsl.* 16: 92–93.

Kitajima, M. and Butler, W.L. (1975) Quenching of chlorophyll fluorescence and photochemistry in chloroplasts by dibromothymoquinone. *Biochim. Biophys. Acta* 376: 105–115.

Knipling, E.B. (1970) Physical and physiological bases for the reflectance of visible and near-infrared radiation from vegetation. *Remote Sens. Environ.* 45: 107–116.

Kobayashi, N., Yanoria, M.J.T. and Fukuta, Y. (2007) Differential varieties bred at IRRI and virulence analysis of blast isolates from the Philippines. *JIRCAS Work Report* 53: 17–30.

Kobayashi, T., Kanda, E., Kitada, K., Ishiguro, K. and Torigoe, Y. (2001) Detection of rice panicle blast with multispectral radiometer and the potential of using airbone multispectral scanners. *Phytopathology* 91: 316–323.

Kobayashi, T., Kanda, E., Naito, S., Nakajima, T., Arakawa, I., Nemoto, K., et al. (2003) Ratio of rice reflectance for estimating leaf blast severity with a multispectral radiometer. *J. Gen. Plant Pathol.* 69: 17–22.

Krause, G.H. and Weis, E. (1991) Chlorophyll fluorescence and photosynthesis: the basics. *Annu. Rev. Plant Physiol. Plant Mol. Biol.* 42: 313–349.

Lenk, S., Chaerle, L., Pfundel, E.E., Langsdorf, G., Hagenbeek, D., Lichtenhaler, H.K., et al. (2007) Multispectral fluorescence and reflectance imaging at the leaf level and its possible applications. *J. Exp. Bot.* 4: 807–814.

Lichtenthaler, H.K. (1987) Chlorophylls and carotenoids: pigments of photosynthetic biomembranes. *Methods Enzymol.* 148: 350–382.

Liu, J.X., Liao, D.Q., Oane, R., Estenor, L., Yang, X.E., Li, Z.C. and Bennett, J. (2006) Genetic variation in the sensitivity of another dehiscence to drought stress in rice. *Field Crops Res.* 97: 87–100.

Luo, C.X., Hanamura, H., Sezaki, H., Kusaba, M. and Yaegashi, H. (2002) Relationship between avirulence genes of the same family in rice blast fungus *Magnaporthe grisea*. *J. Gen. Plant Pathol.* 68: 300–306.

Mahlein, A.K., Steiner, U., Hillnhutter, C., Dehne, H.W. and Oerke, E.C. (2012) Hyperspectral imaging for small-scale analysis of symptoms caused by different sugar beet diseases. *Plant Methods* 8: 3–16.

Maxwell, K. and Johnson, G.N. (2000) Chlorophyll fluorescence—a practical guide. *J. Exp. Bot.* 51: 659–668.

Mew, T.W. (1987) Current status and future prospects of research and bacterial blight of rice. *Annu. Rev. Phytopathol.* 25: 359–382.

Moradi, F. and Ismail, A.M. (2007) Response of photosynthesis, chlorophyll fluorescence and ROS-scavenging systems to salt stress during seedling and reproductive stages in rice. *Ann. Bot.* 99: 1161–1173.

Nedbal, L. and Whitmarsh, J. (2004) Chlorophyll fluorescence imaging of leaves and fruits. *In* Chlorophyll a Fluorescence: A Signature of Photosynthesis. Edited by Papageorgiu, G. and Govindjee. pp. 389–407. Springer, Dordrecht, The Netherlands.

Pandey, S., Bhandari, H. and Hardy, B. (2007) Economic Costs of Drought and Rice Farmers' Coping Mechanisms: A Cross-Country Comparative Analysis. International Rice Research Institute, Manila, Philippines.

Penuelas, J., Filella, I., Biel, C., Serrano, L. and Savé, R. (1993) The reflectance at the 950–970nm region as an indicator of plant water status. *Int. J. Remote Sens.* 14: 1887–1905.

Penuelas, J., Pinol, J., Ogaya, R. and Filella, I. (1997) Estimation of plant water concentration by the reflectance Water Index WI (R900/R970). *Int. J. Remote Sens.* 18: 2869–2875.

Rang, Z.W., Jagadish, S.V.K., Zhou, Q.M., Craufurd, P.Q. and Heuer, S. (2011) Effect of high temperature and water stress on pollen germination and spikelet fertility in rice. *Environ. Exp. Bot.* 70: 58–65.

Rascher, U., Liebig, M. and Luttge, U. (2000) Evaluation of instant light-response curves of chlorophyll-fluorescence parameters obtained with a portable chlorophyll fluorometer on site in the field. *Plant Cell Environ.* 23: 1397–1405.

Rouse, J.W., Haas, R.H., Schell, J.A. and Deering, D.W. (1974) Monitoring vegetation systems in the great plains with ERTS. *In* Third ERTS-1 Symposium. pp. 309–317. Washington, DC.

Schreiber, U., Schliwa, U. and Bilger, W. (1986) Continuous recording of photochemical and non-photochemical chlorophyll fluorescence quenching with a new type of modulation fluorometer. *Photosynth. Res.* 10: 51–62.

Šebela, D., Olejníčková, J., Sotolář, R., Vrchotová, N. and Tříska, J. (2014) Towards optical detection of *Plasmopara viticola* infection in field. *J. Plant Pathol.* 96: 309–320.

Sikuku, P.A., Netondo, G.W., Onzango, J.C. and Musyimi, D.M. (2010) Chlorophyll fluorescence, protein and chlorophyll content of three nerica rainfed rice varieties under varying irrigation regimes. *J. Agric. Biol. Sci.* 5: 19–25.

Song, W.Y., Wang, G.L., Chen, L.L., Kim, H.S., Pi, L., Holsten, T., et al. (1995) A receptor kinase-like protein encoded by the rice disease resistance gene, *Xa21*. *Science* 270: 1804–1806.

Sonti, R.V. (1998) Bacterial leaf blight of rice: new insights from molecular genetics. *Curr. Sci.* 74: 206–212.

Subhash, N. and Mohanan, C.N. (1994) Laser-induced red chlorophyll fluorescence signatures as nutrient stress indicator in rice plants. *Remote Sens. Environ.* 47: 45–50.

Sun, X., Yang, Z., Wang, S. and Zhang, Q. (2003) Identification of a 47-kb DNA fragment containing *Xa4*, a locus for bacterial blight resistance in rice. *Theor. Appl. Genet.* 106: 683–687.

Suriyan, C., Yooyongwech, S. and Supaibulwatana, K. (2010) Water deficit stress in the reproductive stage of four indica rice (*Oryza sativa* L.) genotypes. *Pak. J. Bot.* 42: 3387–3398.

Walther, G.R., Post, E., Convey, P., Menzel, A., Parmesan, C., Beebee, T.J.C., et al. (2002) Ecological responses to recent climate change. *Nature* 416: 389–395.

Wassmann, R., Jagadish, S.V.K., Sumfleth, K., Pathak, H., Howell, G., Ismail, A., et al. (2009) Regional vulnerability of rice production in Asia to climate change impacts and scope for adaptation. *Adv. Agron.* 102: 91–133.

White, J.W., Andrade-Sanchez, P., Gore, M.A., Bronson, K.F., Coffelt, T.A., Conley, M.M., et al. (2012) Field-based phenomics for plants genetic research. *Field Crops Res.* 133: 101–112.

Yang, C. (2010) Assessment of the severity of bacterial leaf blight in rice using canopy hyperspectral reflectance. *Prec. Agric.* 11: 61–81.

Yi, G., Lee, S.K., Hong, Y.K., Cho, Y.C., Nam, M.H., Kim, S.C., et al. (2004) Use of *Pi5(t)* markers in marker-assisted selection to screen for cultivars with resistance to *Magnaporthe grisea*. *Theor. Appl. Genet.* 109: 978–985.

Zagdanska, B. and Kozdoj, J. (1994) Water stress-induced changes in morphology and anatomy of flag leaf of spring wheat. *Acta Soc. Bot. Pol.* 63: 61–66.

Zhang, H., Jin, Q., Chai, R., Hu, H. and Zheng, K. (2010) Monitoring rice leaves blast severity with hyperspectral reflectance. In 2010 2nd International Conference on Information Engineering and Computer Science. pp. 1–4. IEEE.

Zhang, Y.H., Chen, L.J., He, J.L., Qian, L.S., Wu, L.Q. and Wang, R.F. (2010) Characteristics of chlorophyll fluorescence and antioxidative system in super-hybrid rice and its parental cultivar under chilling stress. *Biol. Plant.* 54: 164–168.

Zhou, B., Shaohong, Q., Guifu, L., Maureen, D., Sakai, H., Lu, G., et al. (2006) The eight amino-acids differences within three leucine-rich repeats between *Pi2* and *Piz-t* resistance proteins determine the resistance specificity to *Magnaporthe grisea*. *Mol. Plant Microbe Interact.* 19: 1216–1228.